

Received: 2018.07.25
Accepted: 2018.10.14
Published: 2019.03.20

Anticonvulsant and Neuroprotective Effects of Dexmedetomidine on Pilocarpine-Induced Status Epilepticus in Rats Using a Metabolomics Approach

Authors' Contribution:
Study Design A
Data Collection B
Statistical Analysis C
Data Interpretation D
Manuscript Preparation E
Literature Search F
Funds Collection G

ACDF 1,2 **Xingqin Tan**
ABE 1,2 **Zhenzhen Tu**
BC 1 **Wei Han**
BEF 1 **Xiaojie Song**
CE 1 **Li Cheng**
AF 1 **Hengsheng Chen**
ABC 1,2 **Shengfen Tu**
DF 1,2 **Pan Li**
CF 1,2 **Wei Liu**
AG 1,3 **Li Jiang**

1 Pediatric Research Institute, Children's Hospital of Chongqing Medical University, Ministry of Education Key Laboratory of Child Development and Disorders, China International Science and Technology Cooperation Base of Child Development and Critical Disorders, Chongqing Key Laboratory of Pediatrics, Chongqing, P.R. China
2 Department of Anesthesiology, Children's Hospital of Chongqing Medical University, Chongqing, P.R. China
3 Department of Neurology, Children's Hospital of Chongqing Medical University, Chongqing, P.R. China

Corresponding Author: Li Jiang, e-mail: dr_jiangli@hotmail.com
Source of support: Departmental sources

Background: Status epilepticus (SE) is the most extreme form of seizure. It is a medical and neurological emergency that requires prompt and appropriate treatment and early neuroprotection. Dexmedetomidine (DEX) is mainly used for its sedative, analgesic, anxiolytic, and neuroprotective effects with light respiratory depression. The purpose of this study was to comprehensively analyze the metabolic events associated with anticonvulsion and neuroprotection of DEX on pilocarpine-induced status epilepticus rats by LC-MS/MS-based on metabolomics methods combined with histopathology.

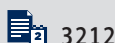
Material/Methods: In this research, rats were divided into 3 groups: a normal group, an SE group, and an SE+DEX group. Hippocampus of rats from each group were collected for further LC-MS/MS-based metabolomic analysis. We collected brains for HE staining and Nissl staining. Multivariate analysis and KEGG enrichment analysis were performed.

Results: Results of metabolic profiles of the hippocampus tissues of rats proved that dexmedetomidine relieved rats suffering from the status epilepticus by restoring the damaged neuromodulatory metabolism and neurotransmitters, reducing the disturbance in energy, improving oxidative stress, and alleviating nucleic acid metabolism and amino acid in pilocarpine-induced status epilepticus rats.

Conclusions: This integral metabolomics research provides an extremely effective method to access the therapeutic effects of DEX. This research will further development of new treats for status epilepticus and provide new insights into the anticonvulsive and neuroprotective effects of DEX on status epilepticus.

MeSH Keywords: **Dexmedetomidine • Metabolomics • Status Epilepticus**

Full-text PDF: <https://www.medscimonit.com/abstract/index/idArt/912283>



3212



1



9



36



Background

Status epilepticus (SE) is the most extreme form of seizure, with abnormal discharge of brain neurons that can change behavior, sensation, and consciousness. The adverse consequences of epileptic seizure are generally neurological deficits, cognitive disorder [1], hippocampal damage, high mortality, and brain edema and ischemia [2]. Therefore, timely, appropriate treatment and early neuroprotective measures are needed to address this neurological emergency. Status epilepticus is associated in insufficient cerebral blood flow, excessive energy consumption, glutamate-mediated excitotoxicity, and destruction of neurotransmitter and neuromodulator metabolism [3]. In clinical practice, intravenous diazepam alone or together with phenytoin, fosphenytoin, and propofol is the standard first-line therapy [4]. In some cases, however, SE rapidly progresses to the refractory stage with prolonged duration [5], and an increased dosage of medication has been associated with adverse effects such as dose-dependent respiratory suppression and hemodynamic changes [6]. Given the high mortality rate of patients with refractory SE, alternative treatments aimed at different targets are needed to alleviate the pathophysiological process.

Dexmedetomidine (DEX), a highly specific central α_2 -adrenoceptor agonist with minimal influence on respiration and hemodynamics [7], has been used in clinical practice for sedation and analgesia, as well as an anxiolytic. DEX can increase the convulsive threshold in cocaine-injected rats [8] and dose-dependently attenuates ropivacaine-induced seizures and negative emotions [9]. In addition, DEX provides neuroprotection against ischemic brain injury by anti-oxidative stress, anti-apoptosis, and inhibiting calcium overload [10]. However, it remains unclear whether DEX is neuroprotective in SE, although DEX had an anticonvulsive effect in a rat model of self-sustaining status epilepticus [11]. The rat SE model induced by lithium-pilo chloride is highly reproducible, with a relatively fixed onset time and a long duration, similar to the human SE formation process, and is one of the more ideal human SE models [12].

Metabolomics has been widely used in the identification of endogenous metabolites. With the rapid expansion of analysis instrument, there are several analytical approaches available for the study of metabolomics, including liquid chromatography/mass spectrometry (LC/MS), gas chromatography/mass

spectrometry (GC/MS), and nuclear magnetic resonance (NMR). In the present study, we first assessed the therapeutic effects of DEX on pilo-induced status epilepticus by using an LC-MS-based metabolomics method. Metabolic profiles were analyzed by multivariate analysis techniques, such as clustering analysis, OPLS-DA, and Volcano Plot. Analysis of significant different metabolomics revealed that there are dramatic changes in various small molecule metabolites in the mouse brain, including stress-reactive oxygen species (ROS), disorders of neurotransmitters and neuromodulators, and disturbances in metabolism of energy substances, nucleic acids, and amino acids. KEGG enrichment revealed the metabolic pathways involved in the anticonvulsant and brain-protective effects of DEX. This research provided clues for further in-depth SE research and therapy.

Material and Methods

Experimental design

Sprague-Dawley (SD) rats (20 days old, SPF, 40–50 g) were randomly divided into 3 groups: a normal group, an SE group, and an SE+DEX group (n=10). Diazepam was used in the experimental groups to stop convulsions, while rats in the normal group were treated with the same volume of normal saline (NS). The rats in the SE+DEX group were intraperitoneally injected with DEX (0.2 $\mu\text{g/g}$) at 60 min, 12 h, 24 h, and 48 h, after SE induction was successfully established. The rats were sacrificed by sodium pentobarbital at 72 h after SE induction, for subsequent experiments. The hippocampal tissues were obtained and rapidly cooled in liquid nitrogen after washing with pre-cooled phosphate-buffered saline (PBS), and then stored at -80°C . Collected samples were transported on dry ice to Shanghai Applied Protein Technology for further metabolomics investigation (Figure 1). Whole brains of rats from each group (n=3) were collected and then fixed in 4% paraformaldehyde and stored at 4°C for further staining. The rats that died or in which SE was not successfully established during the experiments were eliminated from the study and then newly-established SE rats were added.

Status epilepticus rat model

All the rats used in this study were provided by Chongqing Medical University. All the experiments were performed in

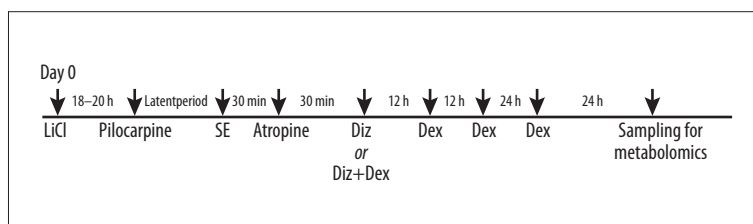


Figure 1. Experimental design sketch of this research. Status epilepticus model was established using LiCl-Pilo induction, and DEX delivery at 60 min, 12 h, 24 h and 48 h after the onset of SE. LiCl, lithium chloride; SE, status epilepticus; Diz, diazepam; DEX, Dexmedetomidine.

accordance with the Animal Ethics Committee of Chongqing Children's Hospital, and all animal procedures were approved by the Laboratory Animal Care Committee of Chongqing Medical University. All rats were housed in a controlled environment (food and water were supplied ad libitum, $21\pm 1^\circ\text{C}$, humidity 60%, 12-h light/dark cycle) [13]. First, the rats were injected intraperitoneally with lithium chloride (127 mg/kg, i.p., Solarbio, Beijing, China). After 18 h, the rats were then intraperitoneally injected with pilocarpine (pilo 30 mg/kg, Sigma) to induce SE. To reduce peripheral effects, the rats were also given an intraperitoneal injection of atropine (1 mg/kg, Shuanghe, Beijing, China) 30 min after SE induction. Diazepam (10 mg/kg, i.p.) was used to stop convulsions at 60 min after SE induction. The rats in the SE or SE+DEX groups that did not exhibit SE were excluded from the study. Convulsions were classified based on the Racine classification system [14]. Rats that had grade IV or V convulsions that lasted for at least 60 min were defined as having SE.

Hematoxylin and Eosin (HE) staining and Nissl staining

After dehydration in gradient alcohol, the fixed tissues were treated with xylene and then embedded with paraffin. These were sectioned into slices (4- μm) and then transferred into a stove at 40°C overnight. Finally, slices were stained with hematoxylin for several minutes, dehydrated in 70% and 90% ethanol, and then stained with eosin for 2–3 min. For Nissl staining, slices were stained with Nissl staining solution for 3–10 mins, then washed with H_2O and 95% ethanol and then dried naturally. Each section was examined under a light microscope.

LC-MS/MS analysis

Total ion current (TIC) and principal component analysis (PCA) to quality control (QC) sample were used to evaluate the stability of the detection system. A QC sample, which was prepared by mixing equal volumes of each sample, was used to validate the method. For TIC, QC samples were loaded, and TIC through UHPLC-Q-TOF MS was obtained, and data chromatographic peaks and retention times were evaluated. For PCA, ion peaks of metabolites from all samples and QC samples were extracted using XCMS software and analyzed using Pareto scaling methods. The system stability was evaluated and the HILIC UHPLC-Q-TOF MS system was imbalanced by analyzing a QC sample. The condition and procedures of LC-MS/MS were explored and performed.

Data analysis and processing

The raw data were transferred into mzXML by ProteoWizard, and data quality was controlled by XCMS. The structure of metabolites was identified by precise mass matching (<25 ppm) and secondary spectrum diagram matching to retrieve the

self-built database. After filtering the data, mode identify was analyzed using SIMCA-P 14.1 (Umetrics, Umea, Sweden) to perform OPLS-DA analysis. Significantly different metabolites were identified based on the combination of a statistically significant threshold of VIP (variable influence on projection) value and a two-tailed t test. Data meeting $\text{VIP} \geq 1$ and $p \leq 0.1$ were considered as significant. KEGG enrichment analysis was performed using MetaboAnalyst (www.metaboanalyst.ca). The volcano plot and clustering analysis were performed using R.

Results

Histopathologic characteristics

HE staining revealed compromised structural integrity of the hippocampal CA1 regions in rats in the SE group. The cells exhibited degeneration, liquefaction, and necrosis. Moreover, the structure of granulos cells was incomplete, and the arrangement of the cells was sparse. However, SE rats treated with DEX exhibited partly intact rat hippocampal CA1 regions (Figure 2A).

We used Nissl staining to investigate the morphology of the rat hippocampal neurons in each group, as shown in Figure 2B. We observed shrinkage and vacuolar cell bodies, as well as cytoplasmic dissolution and interstitial edema, in the hippocampal neurons from SE rats. In contrast, we observed reduced necrotic cells and interstitial edema, and improved morphological structures in hippocampal tissues obtained from SE rats treated with DEX (Figure 2B).

Identification of metabolites

As shown in Figure 3, total ion current chromatograms of metabolites were detected using a solvent system. Accordingly, the relative intensity and peaks under positive mode (Figure 3A) and negative mode (Figure 3B) were different. Nevertheless, we did not observe any obvious differences between QCs, suggesting that variation remained in the optimal range.

Furthermore, the metabolomic data was analyzed by PCA (Figure 4). PCA scatter plots showed a distinct segregation of samples between Nor and SE or SE+DEX. However, a large overlap was found between SE and SE+DEX, indicating a minor influence of DEX on metabolic status from SE.

OPLS-DA analysis, serviced as a supervised method for pattern recognition, was performed on the data in the comparison of SE vs. Nor, SE+DEX vs. SE, and SE+DEX vs. Nor. As shown in Figure 5, groups positive for Nor, SE, and DEX were separated in the OPLS-DA score plots (Figure 5A, 5C, 5E) with a satisfactory goodness of fit ($R^2=0.997$, $Q^2=0.86$ (Figure 5B); $R^2=0.923$, $Q^2=0.699$ (Figure 5D); $R^2=0.999$, $Q^2=0.426$ (Figure 5F)).

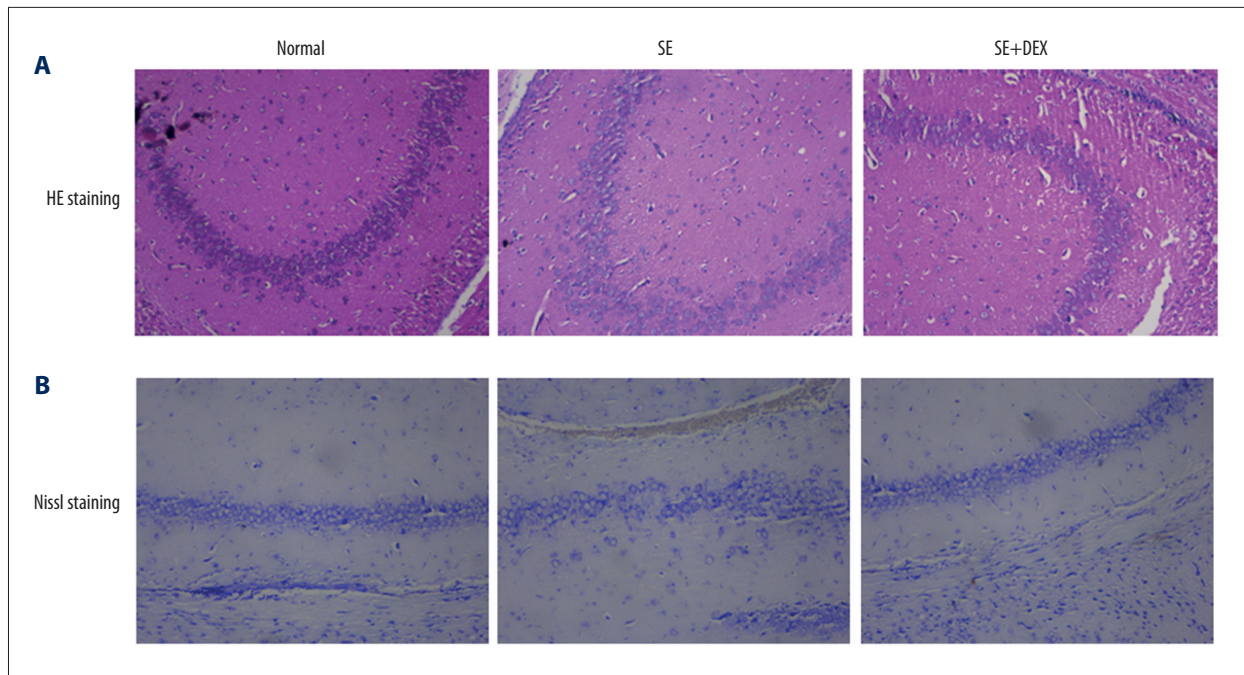


Figure 2. (A, B) Histopathologic characteristics of the rat hippocampus CA1 (hippocampus) area. The changes in hippocampal pathology were detected by HE staining and Nissl staining in rats, from the normal, SE, and SE+DEX groups. Cells presented swelling and lack of Nissl-positive character compared with the Normal group, and histopathologic characteristics recovered after DEX treatment in SE rats.

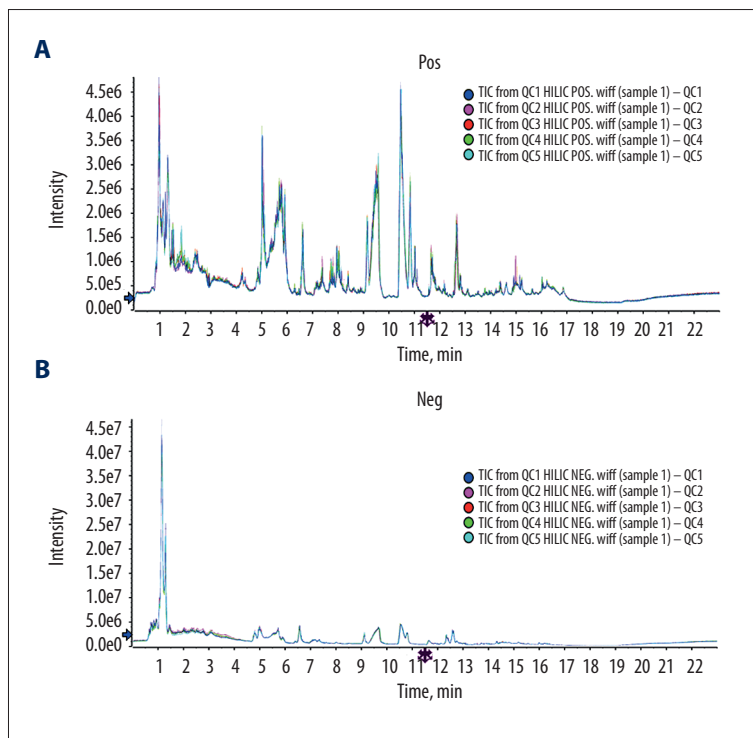


Figure 3. Total ion chromatograms (TIC) of tissue metabolites detected by HILIC under positive (A) and negative (B) ion modes. Metabolomics showed very stable performance as chromatograms were anastomotic in positive ion and negative ion models. QC1~5 indicates n=5 test per modes.

For the metabolites detected under negative mode, score plots for each comparison were also presented as separated clusters (Figure 6A, 6C, 6E), along with optimal goodness of fit ($R^2=0.898$,

$Q^2=0.763$ (Figure 6B); $R^2=0.873$, $Q^2=0.594$ (Figure 6D); $R^2=0.847$, $Q^2=0.164$ (Figure 6F)).

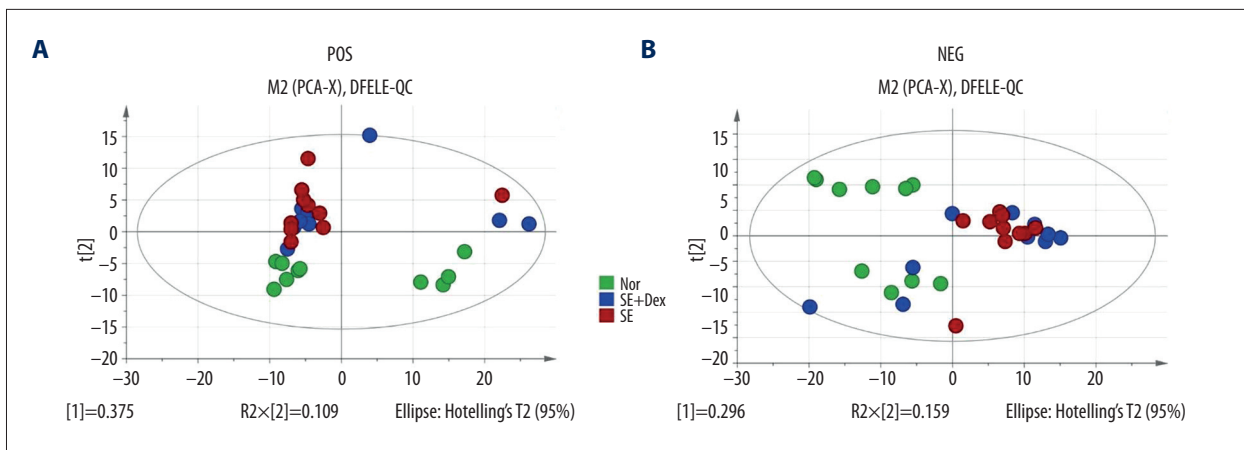


Figure 4. PCA analysis of metabolites by solvent system under positive (A) and negative (B) ion modes. Spots in green show samples from the Normal group; spots in blue indicate samples from the SE+DEX group; Spots in red indicate samples from the SE group.

Analysis of significantly different metabolites

The significantly different metabolites were obtained with VIP >1 between groups. To organized and cluster the significantly different metabolites, two-way hierarchical cluster analysis was performed for comparisons between groups (Figure 7). Results from Figure 7 indicate that the metabolites were highly differentiated among the 3 comparisons.

To further refine the significantly different metabolites, standards of VIP >1 and p value <0.05 were used, and a set of refined metabolites was obtained (Table 1, Figure 8). A total of 11 compounds (e.g., DHAP, F-1,6-BP, glutamate, AR, and GSSG) were retained in Nor, SE, and SE+DEX groups. Of those 11 metabolites, DHAP, F-1,6-BP, glutamate, AR, GSSG, and inosine presented a higher level in SE compared to Nor (Figure 8). Meanwhile, elevated levels of DHAP, F-1,6-BP, glutamate, AR, and inosine were also detected in the SE+DEX group compared with the Nor group. However, when compared with SE, we found obvious suppression of DHAP, F-1,6-BP, glutamate, AR, GSSG, and inosine in the SE+DEX group. Further, we found lower levels of taurine, guanidino butyric acid, SOPC, hypoxanthine AR, and PC (16: 0/16: 0) in the SE group compared with the Nor group, as well as lower levels in the SE+DEX group in comparison with the SE group. We also found that glutamine was higher in the SE group compared with the Nor group, but no significant difference was found between the SE and SE+DEX groups. However, NAAG was significantly lower in the SE+DEX group compared with the SE group (Figure 8A).

We found that levels of ADP, R-5-P, Adenosine, F-6-P, GPC, G-6-P, M-6-P, NANA, and G-1-P were higher in the SE group compared with the Nor group. Meanwhile, ADP, R-5-P, Adenosine, F-6-P, GPC, M-6-P, and G-1-P were also detected at higher levels in the SE+DEX group compared to the Nor group. We found that

the fold change induced by SE was attenuated by DEX. DEX also suppressed NANA to a normal level, as is shown in comparison of SE+DEX vs. Nor. A significant downregulation of ARA was found in the SE group compared with the Nor group, but the fold change induced by SE compared with Nor was obviously reversed by DEX, showing a decrease of fold change when compared with SE+DEX and Nor (Figure 8B).

Lactate and Alpha-D-Glucose were higher in the SE group compared with the Nor group. IMP, AMP, and glyoxylate were downregulated in the SE+DEX group, in contrast to the Nor and SE groups. we found that DHA and NA6P decreased in the SE group compared with the Nor group, but afterwards it was elevated by DEX in the SE+DEX group but not in the SE group. Choline histidine, acetylcholine, deoxycytidine, and threonine were suppressed by DEX in SE rats in comparison with SE (Figure 8C).

KEGG analysis

To reveal the underlying mechanism of SE induced by pilocarpine and ameliorated by DEX, we performed KEGG enrichment analysis. As mentioned above, pilocarpine administration can lead a pathological alteration compared with normal animals. As Figure 9 shows, several pathways are involved. Compared with Nor, Purine metabolism, taurine and hypotaurine metabolism, D-Glutamine and D-glutamate metabolism, GABAergic synapse, long-term depression, FoxO signaling pathway, Fructose and mannose metabolism, and central carbon metabolism in cancer I were enriched in the SE group (Figure 9A). Interestingly, most of the pathways, like long-term depression, GABAergic synapse, Glutathione metabolism, FoxO signaling pathway, and central carbon metabolism in cancer, were also matched in the comparison of SE+DEX vs. Nor or SE+DEX vs. SE (Figure 9B, 9C).

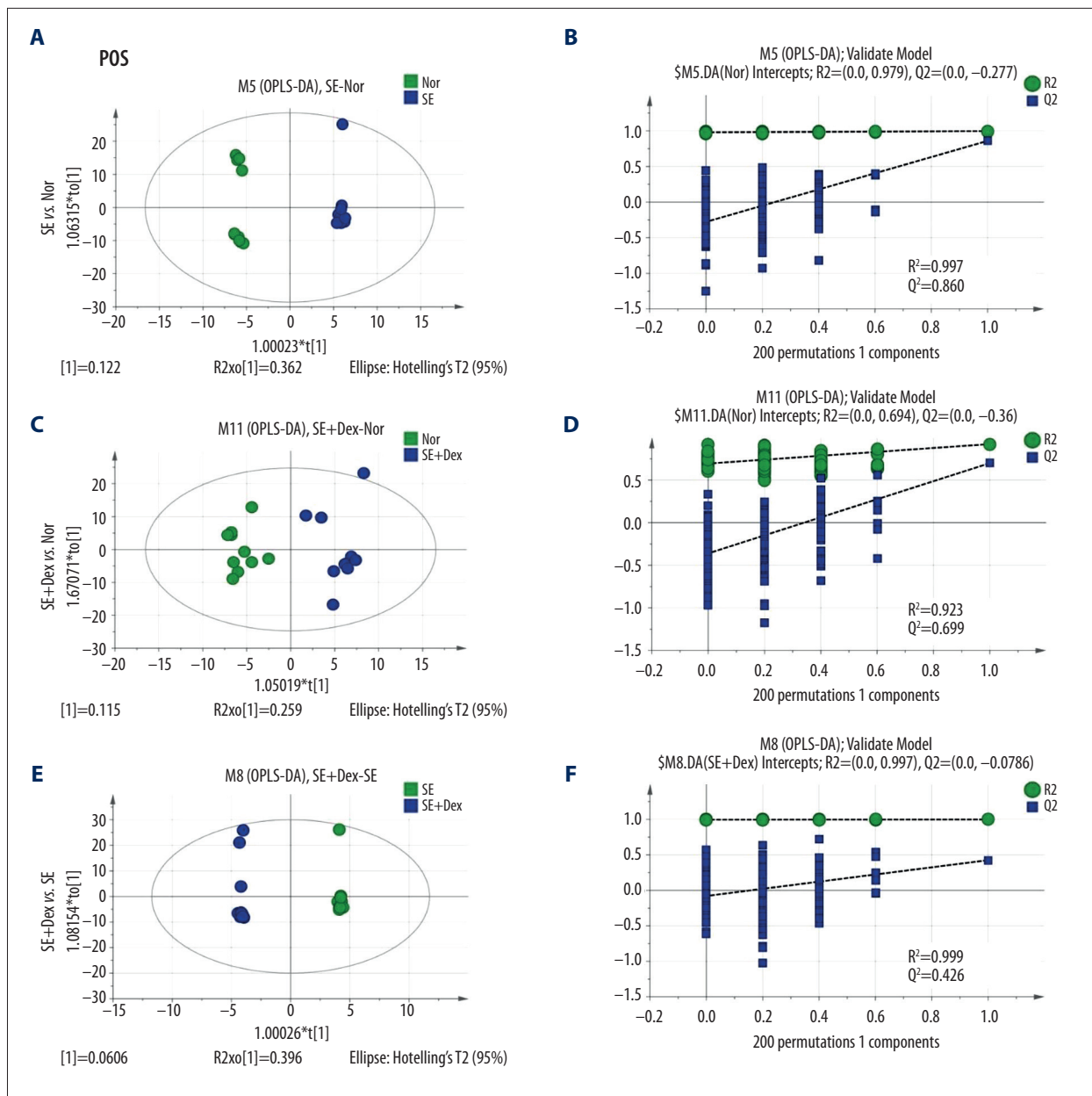


Figure 5. OPLS-DA analysis of LC/MS data from SE vs. Nor (A, B), SE+DEX vs. Nor (C, D), and SE+DEX vs. SE (E, F) under positive mode. Identified compounds could be separated well with optimal goodness of fit. A, C, E: OPLS-DA score plot. B, D, F: Validated model plots obtained by permutation test.

Discussion

Status epilepticus (SE) is one of the most common neurological emergencies in children. Traditionally, SE has been defined as a single epileptic seizure lasting more than 30 min or recurrent seizures without regaining consciousness between seizures for greater than 30 min [15]. Currently, the definition of the duration tends to be shortened to 5 min, emphasizing the importance of early treatment [15–18]. The latency of status epilepticus induced by pilocarpine is generally short and often

accompanied by cognitive impairment and behavioral abnormalities. Therefore, the pilocarpine-induced SE model has been widely accepted by researchers since it can mimic the clinical characteristics of humans in studies of antiepileptic drugs [12]. In the present study, for the first time, dexmedetomidine was used to interfere with a pilocarpine-induced SE model to investigate the anticonvulsant effect and brain-protection effect of dexmedetomidine, a highly selective α_2 receptor blocker, on status epilepticus, characterized by an obvious pathological change observed by HE and Nissl staining. This study has

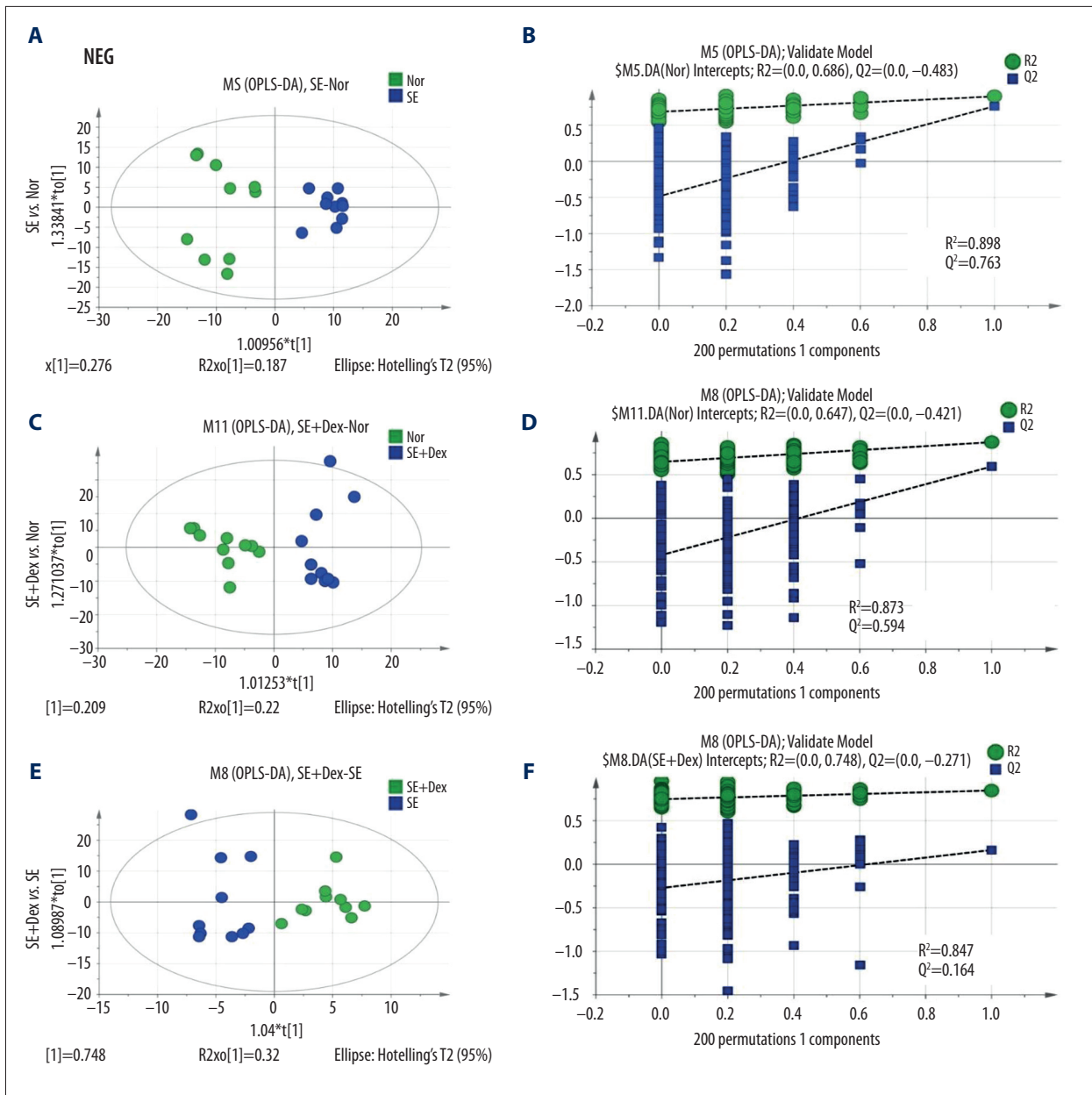


Figure 6. OPLS-DA analysis of LC/MS data from SE vs. Nor (**A, B**), SE+DEX vs. Nor (**C, D**), and SE+DEX vs. SE (**E, F**) under negative mode. Identified compounds can be well-separated with optimal goodness of fit. **A, C, E:** OPLS-DA score plot. **B, D, F:** Validated model plots obtained by permutation test.

important clinical significance and provides new ideas for status epilepticus therapy. LC/MS-based metabolomics is an effective tool for the detection and identification of biomarkers after stimulation of cells or organisms [19]. In this study, we conducted sample preparation, QC examination, LC-MS/MS mass spectrometry, data pretreatment (peak recognition, peak alignment, peak matching), statistical analysis (PCA, PLS-DA, OPLS-DA, t test), differential compound screening and identification, and bioinformatics analysis to explore the therapeutic effect of DEX on SE. In this study, obvious separation was found

between SE vs. Nor and SE+DEX vs. SE (Figures 3–5). However, there was overlap between SE+DEX and Nor or SE+DEX and SE, suggesting DEX might not completely reverse all the SE-induced abnormalities. These observations provide important insights into the novel role of DEX in SE therapy and clinical instructions for further research.

Persistently discharge in neurons in SE can increase cerebral metabolic rate, oxygen consumption, and glucose uptake [20], as well as excess excitatory amino acids release [21,22], creating

Table 1. Identified significant different metabolites from different groups with the VIP and P value.

SE vs. Nor				SE+DEX vs. Nor				SE+DEX vs. SE			
Description	VIP	FC	p value	Description	VIP	FC	p value	Description	VIP	FC	p value
DHAP	2.07	1.84	***	DHAP	2.04	1.55	***	DHAP	1.53	0.84	
F-1,6-BP	3.82	2.20	**	F-1,6-BP	2.76	1.59	*	F-1,6-BP	3.24	0.69	
Glutamate	3.54	1.14	**	Glutamate	4.11	1.10	*	Glutamate	1.38	0.84	
AR	7.92	1.62	***	AR	6.005	1.34	**	AR	5.35	0.83	*
GSSG	1.52	1.18		GSSG	1.45	0.77	**	GSSG	3.58	0.71	**
Inosine	4.82	1.54	*	Inosine	7.57	1.16	*	Inosine	4.26	0.87	*
Taurine	1.76	0.91	*	Taurine	5.80	0.86	**	Taurine	4.39	0.92	
Guanidinobutyric acid	2.37	0.72	**	Guanidinobutyric acid	3.10	0.58	***	Guanidinobutyric acid	1.76	0.80	*
SOPC	1.36	0.58	*	SOPC	1.46	0.87		SOPC	6.61	0.57	**
Hypoxanthine	11.78	0.87		Hypoxanthine	6.90	1.17	*	Hypoxanthine	5.40	0.89	*
PC (16: 0/16: 0)	1.58	0.73		PC (16: 0/16: 0)	1.19	0.76	*	LysoPC(14: 0)	1.39	0.78	
ARA	23.45	0.63	***	ARA	21.28	0.69	***				
ADP	1.11	1.73	***	ADP	1.02	1.54	**	Glyoxylate	1.96	0.74	
R-5-P	1.70	2.51	**	R-5-P	1.69	2.02	*	NA6P	2.12	2.42	*
Adenosine	1.27	1.59	*	Adenosine	1.47	1.51	**	Threonate	2.92	0.70	
F-6-P	2.36	2.45		F-6-P	3.31	2.14	*	Choline	2.30	0.78	*
GPC	7.33	3.33	**	GPC	8.37	3.26	***	Histidine	2.46	0.73	*
G-6-P	2.93	1.72	*	G-6-P	1.33	2.49	*	Acetylcholine	2.13	0.77	
M-6-P	2.78	2.42		M-6-P	1.99	1.89	*	Deoxycytidine	1.30	0.69	***
NANA	1.04	2.09		NANA	1.43	0.83	*				
G-1-P	2.76	2.17		G-1-P	1.48	1.47	**				
Glutamine	3.90	1.15						NAAG	2.57	0.84	
Glucose	1.05	4.23	*	IMP	1.31	0.58	**	IMP	2.10	0.63	**
Lactate	1.57	1.35	*	AMP	1.09	0.75	*	AMP	1.50	0.81	*
DHA	2.81	0.91						DHA	4.50	1.12	
MA	2.43	1.17	*	Glyoxylate	2.18	0.51	**				

GSSG – glutathione disulfide; DHAP – dihydroxyacetone phosphate; ARA – arachidonic acid; DHA – docosahexaenoic acid; ADP – adenosine 5'-diphosphate; IMP – inosine 5'-monophosphate; AMP – adenosine monophosphate; SOPC – 1-Stearoyl-2-oleoyl-sn-glycerol 3-phosphocholine; F-1,6-BP – fructose 1,6-bisphosphate; NANA – N-acetylneuraminic acid; R-5-P – ribose 5-phosphate; GPC – glycerophosphocholine; AR – allopurinol riboside; NAG6P – N-acetyl-D-glucosamine 6-phosphate; MA – malic acid; FC – fold change; * P<0.05, ** p<0.01, *** p<0.001 vs. groups.

an imbalance with inhibitory neurotransmitters, and causing excitotoxicity [23], oxidative stress [24], calcium overload [25], neuronal apoptosis [26], and other brain damage. In this study, the excitatory amino acid glutamine, was significantly

increased in the SE group compared with that in the normal group, while taurine, an inhibitory neurotransmitter [27], was significantly reduced, and the high energy metabolism and oxidative stress [28] markers, such as DHAP, F-1,6-BP, AR, GSSG,

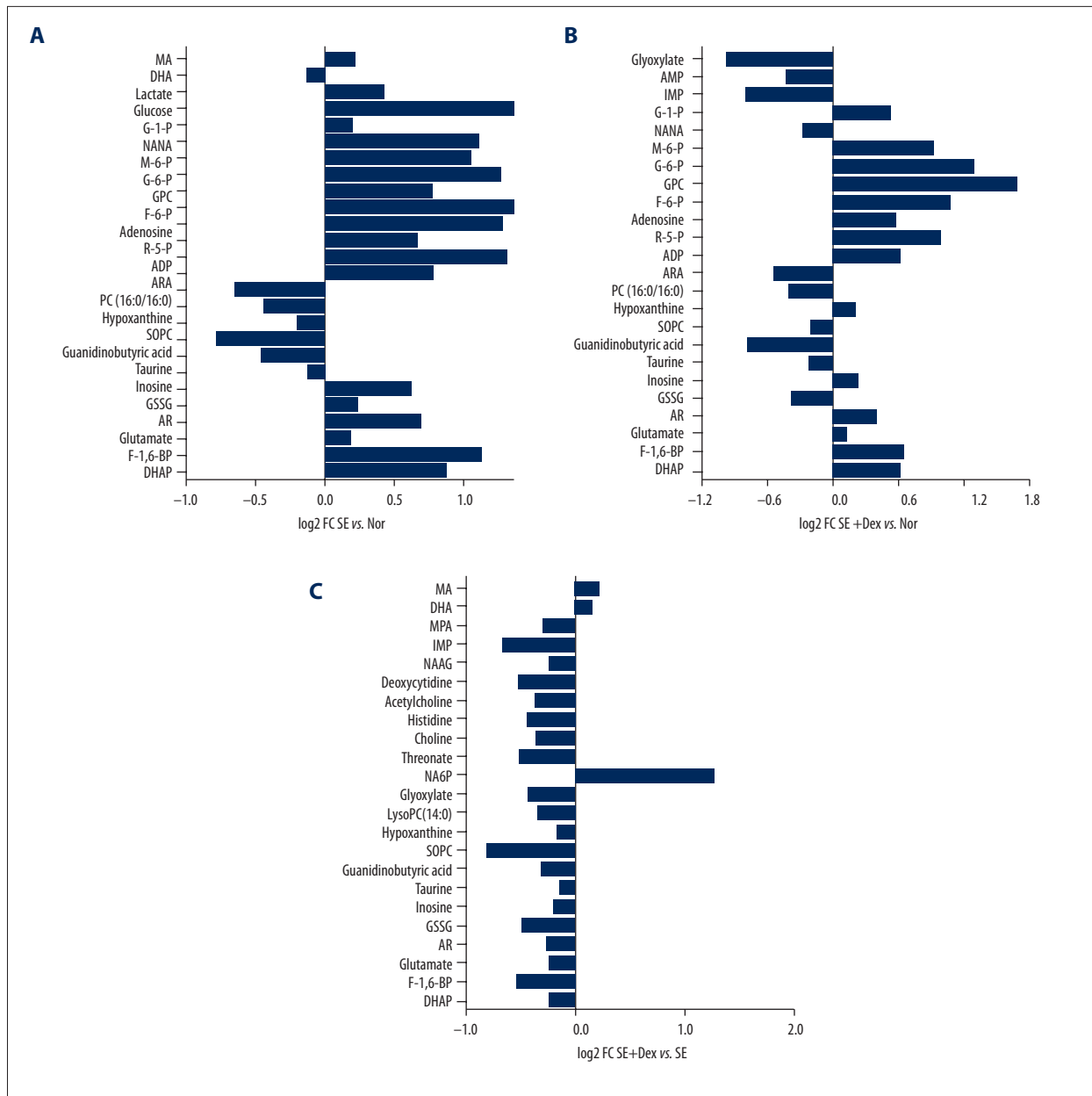


Figure 8. Significantly different metabolites between groups plotted with fold change plots based on $p < 0.05$ and $VIP > 1$. (A) Shows metabolites with significant difference between SE and Nor. (B) Shows metabolites with significant difference between SE+DEX and Nor. (C) Shows metabolites with significant difference between SE+DEX and SE.

inosine, ADP, R-5-P, Adenosine, F-6-P, GPC, G-6-P, M-6-P, NANA, G-1-P, Lactate, Alpha-D-Glucose, and MA, were significantly increased. Guanidinobutyric acid is a precursor of L-arginine, which was significantly reduced in the model group and is associated with the synthesis of the NO in the brain [29]. The alteration of guanidino butyric acid observed in this study suggests that SE causes brain damage by inhibiting the synthesis of NO, similar to the findings of a previous study [30]. SOPC, hypoxanthine [31], and PC (16: 0/16: 0) [32] are involved in the synthesis of sphingolipids, and are also involved in cell growth,

differentiation, and apoptosis, which is important in ensuring the integrity of cell membranes. In this study, there was a significant decrease of these metabolites in the model group, suggesting neuronal apoptosis or death in SE might be caused by SOPC, hypoxanthine, and PC (16: 0/16: 0). ARA and DHA are brain-protective substances that are indispensable for brain and nerve development [33,34], and these 2 metabolins were significantly reduced in the model group, suggesting cognitive impairment in animals in the model group. These changes were similar to the pathophysiological changes that occurred

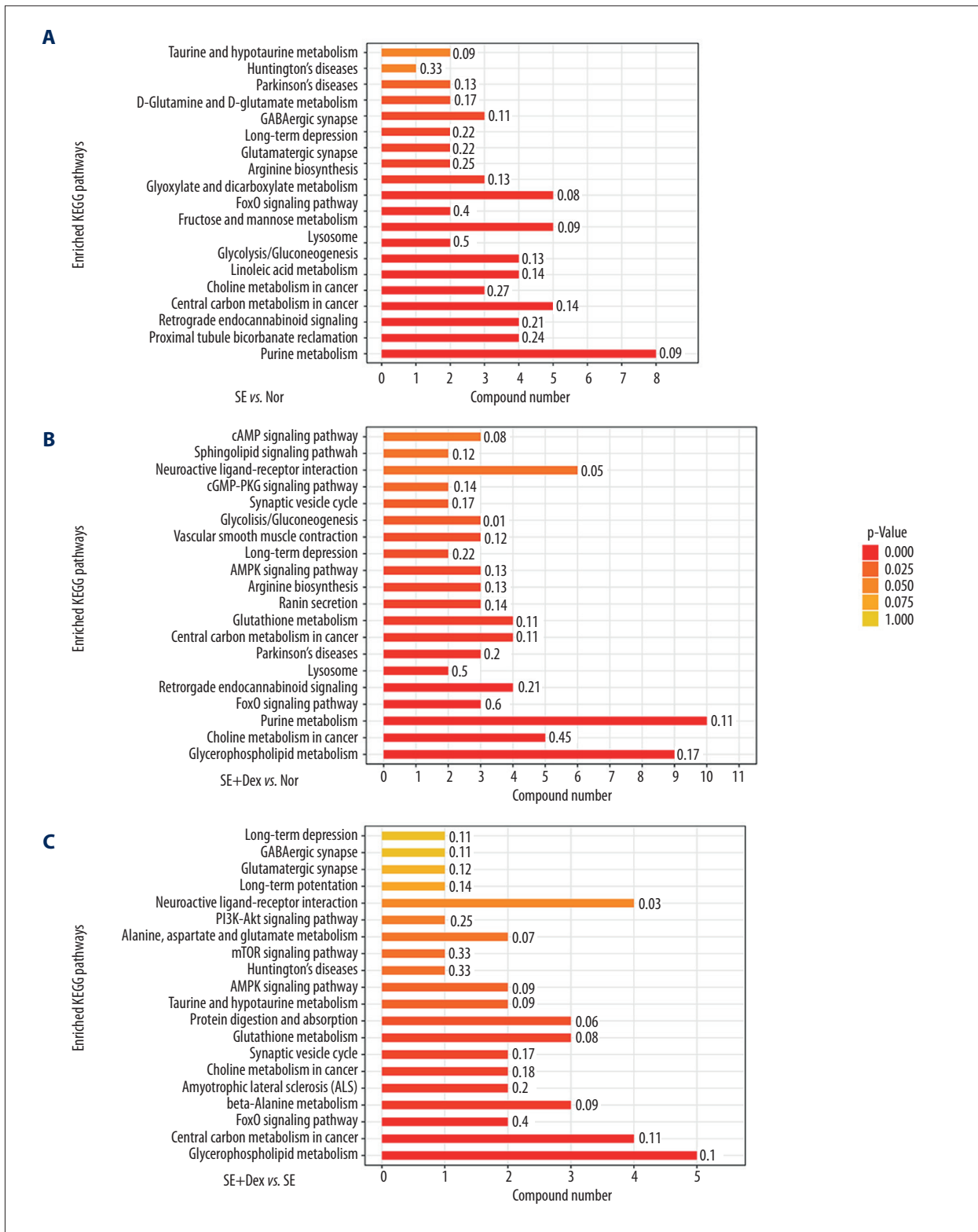


Figure 9. Enriched KEGG pathways based on significant different metabolites between SE and Nor (A), SE+DEX and Nor (B), and SE+DEX and SE (C). Purine metabolism, Taurine and hypotaurine metabolism, D-glutamine and D-glutamate metabolism, GABAergic synapse, and long-term depression were involved in rats with SE, and DEX can restore the symptoms through those pathways.

during status epilepticus, demonstrating the successful establishment of the model.

DEX has been proved to function on anti-oxidative stress and inhibit glutamate release, resisting epilepsy, and protecting the brain against SSE [11]. In this study, our observation of DEX delivery confirmed this. DEX-intervention can modulate the level of glutamate, DHAP, F-1,6-BP, AR, GSSG, inosine, ADP, R-5-P, adenosine, F-6-P, GPC, M-6-P, NANA, G-1-P, Guanidinobutyric acid, hypoxanthine, PC (16: 0/16: 0), and ARA, suggesting that after dexmedetomidine intervention, the high post-epileptic metabolic rate, oxidative stress impairment, and neuronal apoptosis were reduced in the model. In addition, changes in excitatory amino acids caused by DEX may also be involved in brain protection and antiepileptic mechanisms. Specifically, the excitatory amino acids such as glutamate and NAAG in SE animals with DEX were significantly lower than those in the model group, and the inhibitory amino acid taurine was also significantly reduced, which may be related to the decrease of glutamate and thus blocked the synthesis of inhibitory amino acids. DEX can increase DHA and NA6P to take part in post-epilepsy brain protection. It suggested that dexmedetomidine's effect of brain protection was mainly achieved by inhibiting excitatory amino acids. Other indicators of high energy and oxidative stress, such as DHAP, F-1,6-BP, AR, GSSG, and inosine, were significantly reduced compared in the model group, suggesting that DEX attenuated the metabolic rate and oxidative stress injury in the model group.

KEGG is one of the most commonly used bioinformatics databases in the world. It is widely used for understanding advanced function, biological system genome sequencing, and other high-throughput experimental techniques. The results of KEGG enrichments in this study suggest that the pilocarpine-induced epilepticus model led to pathophysiological processes through D-Glutamine and D-glutamate metabolism, alanine, aspartate, and glutamate metabolism, GABAergic synapse, Glutamatergic synapse, and taurine and hypotaurine metabolism. Sustained epileptic discharge and neurotoxicity of excitatory amino acids were related to the imbalance between

excitatory neurotransmitter and inhibitory neurotransmitter; Central carbon and Choline metabolism in cancer, Glyoxylate and dicarboxylate metabolism, suggesting high metabolism, anaerobic glycolysis, oxidative stress, and other pathophysiological processes of the SE model. Huntington's disease, Parkinson's disease, chronic depression, and retrograde endocannabinoid signaling suggest that SE causes brain degenerative changes and changes in cognitive function [35,36]. The reliability of the SE model in this experiment was further confirmed. Comparison of the SE+DEX group with the normal group shows that DEX may play a role by participating in FoxO and other signaling pathways. In addition, FoxO and other signaling pathways were also pre-concentrated, suggesting that DEX exerts its therapeutic effect in these ways.

Conclusions

In this study, SE rats were established and subsequently managed with diazepam and DEX. The pathological features of these rats were significantly relieved after treatment with DEX. Our metabolomics approach revealed several compounds – glutamate, GSSG, taurine, and SOPC – involved with balance of excitatory amino acids and regulation of metabolic rate, and these results show the function of DEX in epileptic rats. Observations from the KEGG analysis suggest that DEX plays a role in brain protection and antioxidant stress in the pilocarpine-induced SE model. Future work needs to focus on further characterizing the functions of these metabolites to help develop more effective targets for SE therapy.

Acknowledgements

Medical writer and editor, Pranali P Pathare, PhD (3P Scientific Communications) provided English language editing of this manuscript.

Conflict of interest

None.

References:

1. Zhang Q, Ding D, Zhou D et al: Cognitive dysfunction in people with convulsive seizures in rural China. *Epilepsy Behav*, 2012; 24(4): 435–38
2. Raspall-Chaure M, Chin RF, Neville BG, Scott RC: Outcome of paediatric convulsive status epilepticus: a systematic review. *Lancet Neurol*, 2006; 5: 769–79
3. Fauvel F, Dorandeu F, Carpentier P et al: Changes in mouse brain metabolism following a convulsive dose of soman: A proton HRMAS NMR study. *Toxicology*, 2010; 267: 99–111
4. Fung EL, Fung BB: Review and update of the Hong Kong Epilepsy Guideline on status epilepticus. *Hong Kong Med J*, 2017; 23: 67–73
5. Mazarati AM, Baldwin RA, Sankar R, Wasterlain CG: Time-dependent decrease in the effectiveness of antiepileptic drugs during the course of self-sustaining status epilepticus. *Brain Res*, 1998; 814: 179–85
6. Trinka E: The use of valproate and new antiepileptic drugs in status epilepticus. *Epilepsia*, 2010; 48: 49–51
7. Hoffman WE, Kochs E, Werner C et al: Dexmedetomidine improves neurologic outcome from incomplete ischemia in the rat. Reversal by the alpha 2-adrenergic antagonist atipamezole. *Anesthesiology*, 1991; 75: 328–32
8. Whittington RA, Virag L, Vulliamoz Y et al: Dexmedetomidine increases the cocaine seizure threshold in rats. *Anesthesiology*, 2002; 97: 693–700
9. Zhai MZ, Wu HH, Yin JB et al: Dexmedetomidine dose-dependently attenuates ropivacaine-induced seizures and negative emotions via inhibiting phosphorylation of amygdala extracellular signal-regulated kinase in mice. *Mol Neurobiol*, 2016; 53: 2636–46

10. Akpınar H, Nazıroğlu M, Övey İ et al: The neuroprotective action of dexmedetomidine on apoptosis, calcium entry and oxidative stress in cerebral ischemia-induced rats: Contribution of TRPM2 and TRPV1 channels. *Sci Rep*, 2016; 6: 37196
11. Kan MC, Wang WP, Yao GD et al: Anticonvulsant effect of dexmedetomidine in a rat model of self-sustaining status epilepticus with prolonged amygdala stimulation. *Neurosci Lett*, 2013; 543: 17–21
12. Cavalheiro EA, Santos NF, Priel MR: The pilocarpine model of epilepsy in mice. *Epilepsia*, 2010; 37: 1015–19
13. Joshi S, Rajasekaran K, Hawk KM et al: Status epilepticus: Role for etiology in determining response to benzodiazepines. *Ann Neurol*, 2018; 83(4): 830–41
14. Racine RJ: Modification of seizure activity by electrical stimulation. II. Motor seizure. *Electroencephalogr Clin Neurophysiol*, 1972; 32: 281–94
15. Abend NS, Lodenkemper T: Pediatric status epilepticus management. *Curr Opin Pediatr*, 2014; 26: 668–74
16. Tasker RC: Status epilepticus in children. *Curr Opin Pediatr*, 2014; 26: 653–54
17. Trinka E, Cock H, Hesdorffer D et al: A definition and classification of status epilepticus – Report of the ILAE Task Force on Classification of Status Epilepticus. *Epilepsia*, 2015; 56: 1515–23
18. Ng YT, Maganti R: Status epilepticus in childhood. *J Paediatr Child Health*, 2013; 49: 432–37
19. Trushina E: Advanced LC-MS applications in metabolomics. In: Han J, Parker C, Borchers C (eds.), *LC-MS-based metabolomics in understanding the mechanisms of Alzheimer's disease and biomarker discovery*. London, UK, Future Science; 2015: 40–57
20. Li P, Wei DD, Wang JS et al: (1)H NMR metabolomics to study the effects of diazepam on anisatin induced convulsive seizures. *J Pharm Biomed Anal*, 2016; 117: 184–94
21. Costa MS, Rocha JB, Perosa SR et al: Pilocarpine-induced status epilepticus increases glutamate release in rat hippocampal synaptosomes. *Neurosci Lett*, 2004; 356: 41–44
22. Ueda Y, Yokoyama H, Nakajima A et al: Glutamate excess and free radical formation during and following kainic acid-induced status epilepticus. *Exp Brain Res*, 2002; 147: 219–26
23. Kim SH, Bae HR, Kim SW: Topiramate prevents glutamate receptor-mediated astrocyte excitotoxicity in pilocarpine-induced status epilepticus mice. 15th Meeting of the European-Neurological-Society; 2005 June; 2005
24. Shin EJ, Jeong JH, Chung YH et al: Role of oxidative stress in epileptic seizures. *Neurochem Int*, 2011; 59: 122–37
25. Amano H, Amano T, Matsubayashi H et al: Enhanced calcium influx in hippocampal CA3 neurons of spontaneously epileptic rats. *Epilepsia*, 2010; 42: 345–50
26. Hu Y, Jiang L, Li X, Zhang XP: [Correlative factors of neuronal apoptosis in hippocampus after status convulsion.] *Chinese Journal of Neurology*, 2006; 39: 36–38 [in Chinese]
27. Albrecht J, Schousboe A: Taurine interaction with neurotransmitter receptors in the CNS: An update. *Neurochem Res*, 2005; 30: 1615–21
28. Izumi Y, Benz AM, Katsuki H et al: Effects of fructose-1,6-bisphosphate on morphological and functional neuronal integrity in rat hippocampal slices during energy deprivation. *Neuroscience*, 2003; 116: 465–75
29. Ratnakumari L, Qureshi IA, Butterworth RF et al: Arginine-related guanidino compounds and nitric oxide synthase in the brain of ornithine transcarbamylase deficient spf mutant mouse: Effect of metabolic arginine deficiency. *Neurosci Lett*, 1996; 215: 153–56
30. Nozaki K, Moskowitz MA, Maynard KI et al: Possible origins and distribution of immunoreactive nitric oxide synthase-containing nerve fibers in cerebral arteries. *J Cereb Blood Flow Metab*, 1993; 13: 70–79
31. Bangaru ML, Park F, Hudmon A et al: Quantification of gene expression after painful nerve injury: Validation of optimal reference genes. *J Mol Neurosci*, 2012; 46: 497–504
32. Kugler W, Erdlenbruch B, Jünemann A et al: Erucylphosphocholine-induced apoptosis in glioma cells: Involvement of death receptor signalling and caspase activation. *J Neurochem*, 2010; 82: 1160–70
33. Saitoh M, Nagai K, Yaguchi T et al: Arachidonic acid peroxides induce apoptotic Neuro-2A cell death in association with intracellular Ca(2+) rise and mitochondrial damage independently of caspase-3 activation. *Brain Res*, 2003; 991: 187–94
34. Ohuchi K, Ono Y, Joho M et al: A docosahexaenoic acid-derived pro-resolving agent, Maresin 1, protects motor neuron cells death. *Neurochem Res*, 2018; 43: 1413–23
35. Braunewell KH, Manahanvaughan D: Long-term depression: A cellular basis for learning? *Rev Neurosci*, 2001; 12: 121–40
36. Fitzjohn SM, Palmer MJ, May JE et al: A characterisation of long-term depression induced by metabotropic glutamate receptor activation in the rat hippocampus *in vitro*. *J Physiol*, 2010; 537: 421–30